Supporting Information: Programmable Functionalization of Surfactant-Stabilized Microfluidic Droplets via DNA-Tags

Kevin Jahnke,[†,‡] Marian Weiss,[†,‡] Christoph Frey,[†,‡] Silvia Antona,[†,‡] Jan-Willi Janiesch,[†,‡] Ilia Platzman,[†,‡] Kerstin Göpfrich,[*,†,‡] and Joachim P. Spatz[*,†,‡]

†*Max Planck Institute for Medical Research, Department of Cellular Biophysics, Jahnstraße 29, D 69120, Heidelberg, Germany*

‡*Department of Biophysical Chemistry, University of Heidelberg, Im Neuenheimer Feld 253, D 69120 Heidelberg, Germany*

E-mail: kerstin.goepfrich@mpimf-heidelberg.mpg.de; spatz@mr.mpg.de

Contents

Table S1: DNA sequences

Supporting Table 1: DNA sequences. The column on the far-right indicates the experiments that the DNA was used for.

#	DNA sequence	Fig.
1	5'Cy3 (or Atto488)/TTCCTTCTATGCATCA/3'CholTEG	1b,e; 2; 3d
2	TCTATGCATCA/3'Atto488	1c,f
3	5'Atto488/TGATGCATAGAAGGAA/3'Amine	3a
4	i: 5'Atto488/GCTCGAGCCAGTGAGGACGGAAGTTTGTCGTAGCATCGCACC ii: GCTCGAGCCAACCACGCCTGTCCATTACTTCCGTCCTCACTG/3'CholTEG iii: GCTCGAGCGGTGCGATGCTACGACTTTGGACAGGCGTGGTTG	3b
5	ACCAGACAATACCACACAATTTT/3'CholTEG/	3d
6	5'Atto488/TTCTCTTCTCGTTTGCTCTTCTCTTGTGTGGTATT GTCTAAGAGAAGAGTT/3'BioTEG/	3d
7	CTACTATGGCGGGTGATAAAAAACGGGAAGAGCATGCC CATCCAA/3CholTEG	3c,e
8	5'FITC/GGATGGGCATGCTCTTCCCGTTTTTTATCACCCGC CATAGTAGGAGGTAAGTTATGACAGGTCCA	3c,e
9	5'Cy5/GGATGGGCATGCTCTTCCCGTTTTTTATCACCCG CCATAGTAGAGGACCTGTCATAACTTACCTG	3c,e
10	5'Atto488/TTCCTTCTATGCATCA/3'CholTEG	4
11	TCTATGCATCA/3'ROX	4

Figure S1: Design and assembly of the DNA lattice

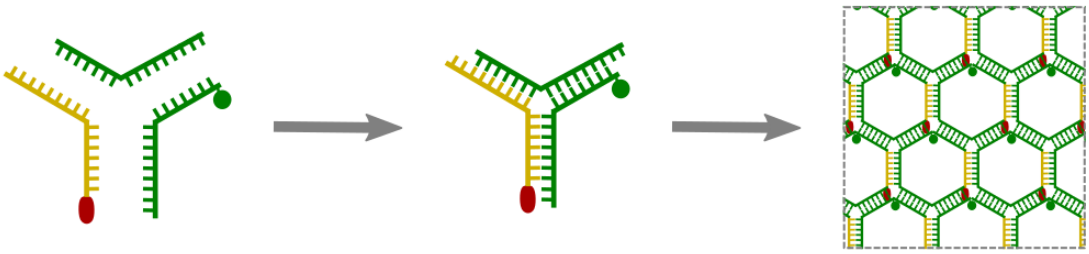

Supporting Figure 1: Schematic illustration of the DNA lattice design, adapted from Kurokawa *et al.*[1] The lattice is composed of three DNA sequences (see Table S1, #4) with sticky ends for polymerization into hexagonal lattices. One of the DNA strands has a 3' cholesterol tag (red, oval shape), another is tagged with Atto488 (green circle). The lattice was assembled by mixing the three strands at equimolar concentrations of 2 µM in a buffer containing 10 mM Tris, 1 mM EDTA and 10 mM $MgCl_2$. The mixture was annealed in a thermocycler (Biorad) by heating to 60 °C for 10 minutes and subsequently encapsulated into microfluidic droplets via the aqueous phase.

Figure S2: Design and fabrication of the microfluidic devices

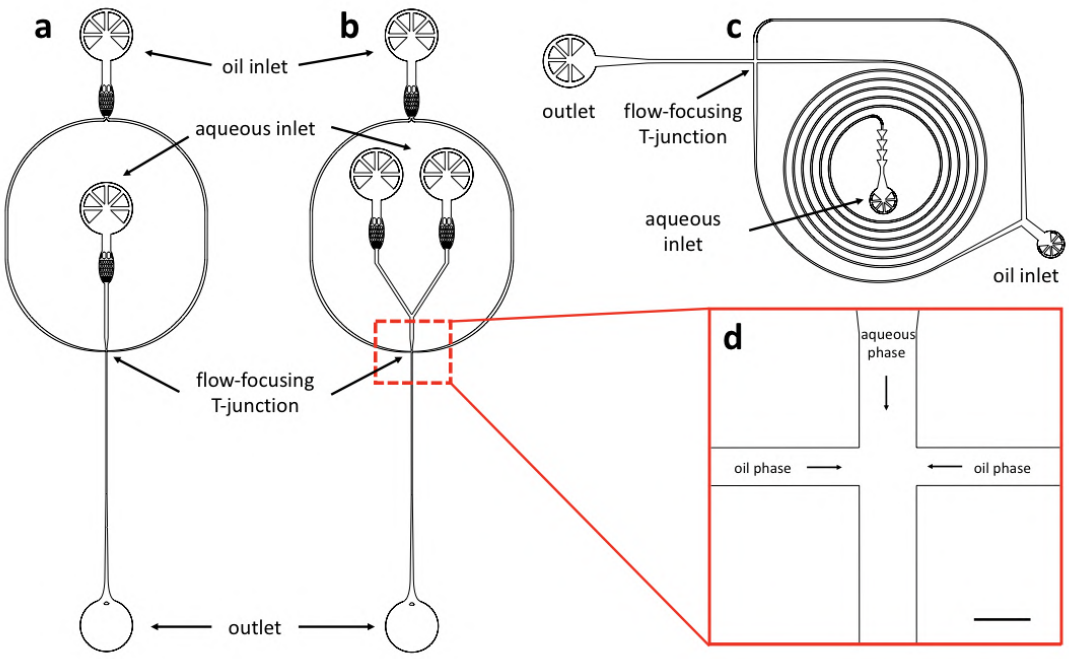

Supporting Figure 2: Layout of microfluidic devices for the production of surfactant-stabilized droplets. a) Device with one oil-inlet and one water-inlet used for the encapsulation of cholesterol-tagged DNA as well as the joint encapsulation of cholesterol-tagged and complementary DNA (amine-tagged, cholesterol-tagged, fluorescently-labeled DNA and the DNA lattice); b) Device with one oil-inlet and two water-inlets used for actin and bead encapsulation with DNA. The cholesterol-tagged DNA was supplied via one inlet and the respective complementary DNA strands via the second one to avoid aggregation prior to droplet formation; c) Device with a coiled water inlet used for Jurkat cell encapsulation. The coil provides better separation of the cells. The microfluidic PDMS devices (Sylgard 184, Dow Corning, USA) were fabricated according to a previously published protocol.[2] For confocal imaging, the droplets were collected from the outlet and sealed in a simple observation chamber as described previously.[3]

Figure S3: Water-in-oil vs. oil-in-water droplets with DNA

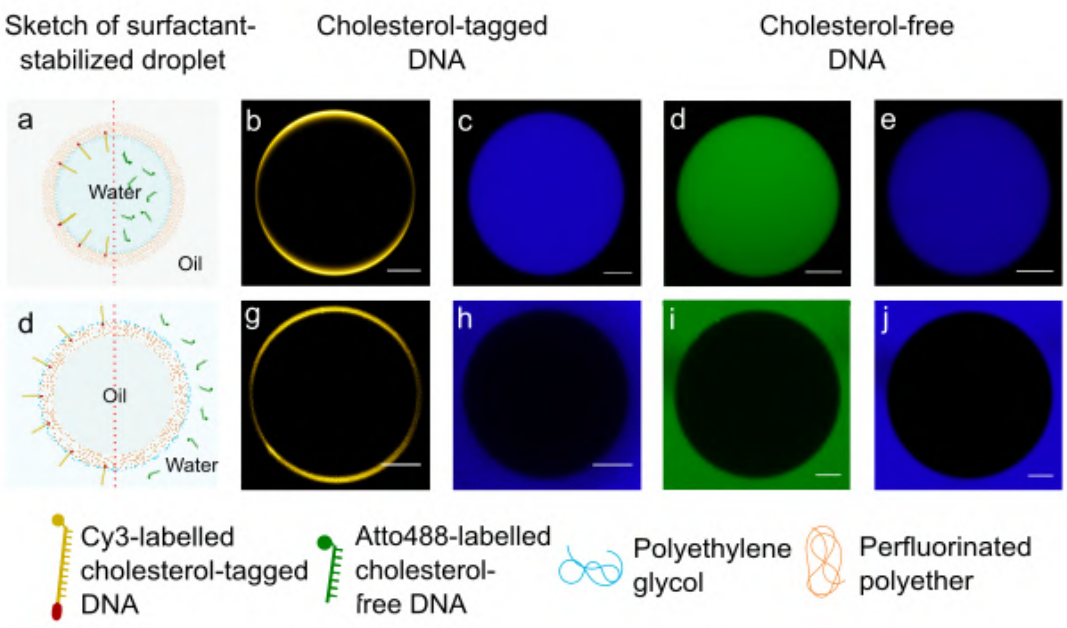

Supporting Figure 3: Interaction of cholesterol-tagged and cholesterol-free DNA with surfactant-stabilized droplets employing a fluorescence labeled aqueous phase. a) Schematic illustration of a water-in-oil droplet (left of dotted red line: with cholesterol-tagged DNA, right side: with cholesterol-free DNA); b,d) Confocal fluorescence images of a water-in-oil droplet with cholesterol-tagged Cy3-labeled DNA (λ_{ex} = 550nm) (b) or cholesterol-free Atto488-labeled DNA (λ_{ex} = 488nm) (d) in the internal aqueous phase; c,e) Aqueous phase labeled via dissolving an Alexa405 dye (λ_{ex} = 405nm) for droplets containing cholesterol-tagged DNA (c) or cholesterol-free DNA (e) in the internal aqueous phase; f) Schematic illustration of an oil-in-water droplet (left of dotted red line: with cholesterol-tagged DNA, right side: with cholesterol-free DNA), g,i) Confocal fluorescence images of an oil-in water droplet with cholesterol-tagged Cy3-labeled DNA (g) and cholesterol-free Atto488-labeled DNA (i) in the external aqueous phase; h,j) aqueous phase labeled via an Alexa405 dye for cholesterol-tagged DNA (g) and cholesterol-free DNA (i) in the external aqueous phase. Whereas cholesterol-tagged DNA self-assembles at the droplet periphery, cholesterol-free DNA remains homogenously distributed in the aqueous phase, which consisted of 10 mM Tris-HCl, 1 mM EDTA, 5 mM $MgCl_2$, 1 per mille Alexa405 dye (Thermo Fisher Scientific), pH 8. Scale bars: 10 µm.

Figure S4: Fluorescent intensity profiles of droplets

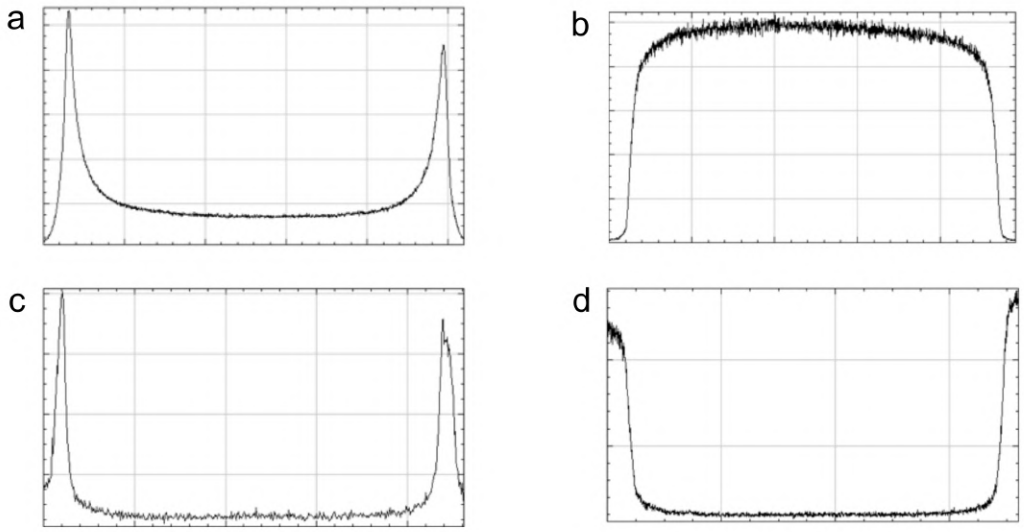

Supporting Figure 4: Intensity profiles of cholesterol-tagged and cholesterol-free water-in-oil and oil-in-water droplets. Fluorescence intensity profile for a) cholesterol-tagged Cy3-labeled ($\lambda_{ex} = 561$nm) DNA attached to a water-in-oil droplet, b) cholesterol-free Atto488-labeled ($\lambda_{ex} = 488$nm) DNA inside a water-in-oil droplet, c) cholesterol-tagged Cy3-labeled ($\lambda_{ex} = 561$nm) DNA attached to an oil-in-water droplet, d) cholesterol-free Atto488-labeled ($\lambda_{ex} = 488$nm) DNA outside of an oil-in-water droplet. The corresponding images can be seen in Figure 1

Figure S5: Fluorophore-independent interaction of cholesterol-tagged DNA

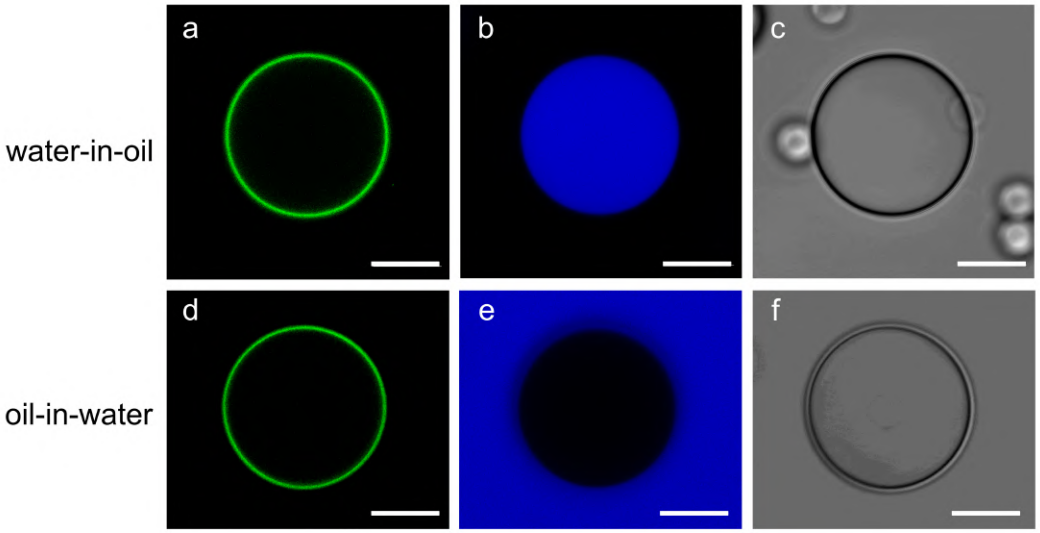

Supporting Figure 5: Interaction of cholesterol-tagged Atto488-labeled DNA with surfactant-stabilized droplets. a,b) Confocal fluorescence images of a water-in-oil droplet with cholesterol-tagged Atto488-labeled DNA (λ_{ex} = 488nm) (a) or an Alexa405 dye (λ_{ex} = 405nm) to label the aqueous phase (b); c) the corresponding brightfield image; confocal fluorescence images of an oil-in-water droplet with cholesterol-tagged Atto488-labeled DNA (λ_{ex} = 488nm) (d) or an Alexa405 dye (λ_{ex} = 405nm) to label the aqueous phase (e); f) the corresponding brightfield image. Cholesterol-tagged Atto488-labeled DNA assembles at the droplet periphery with an aqueous phase consisting out of 10 mM Tris-HCl, 1 mM EDTA, 5 mM $MgCl_2$, 10 µM Alexa405 dye, pH8. Scale bars: 30 µm.

Figure S6: Influence of divalent cations on DNA-surfactant interaction

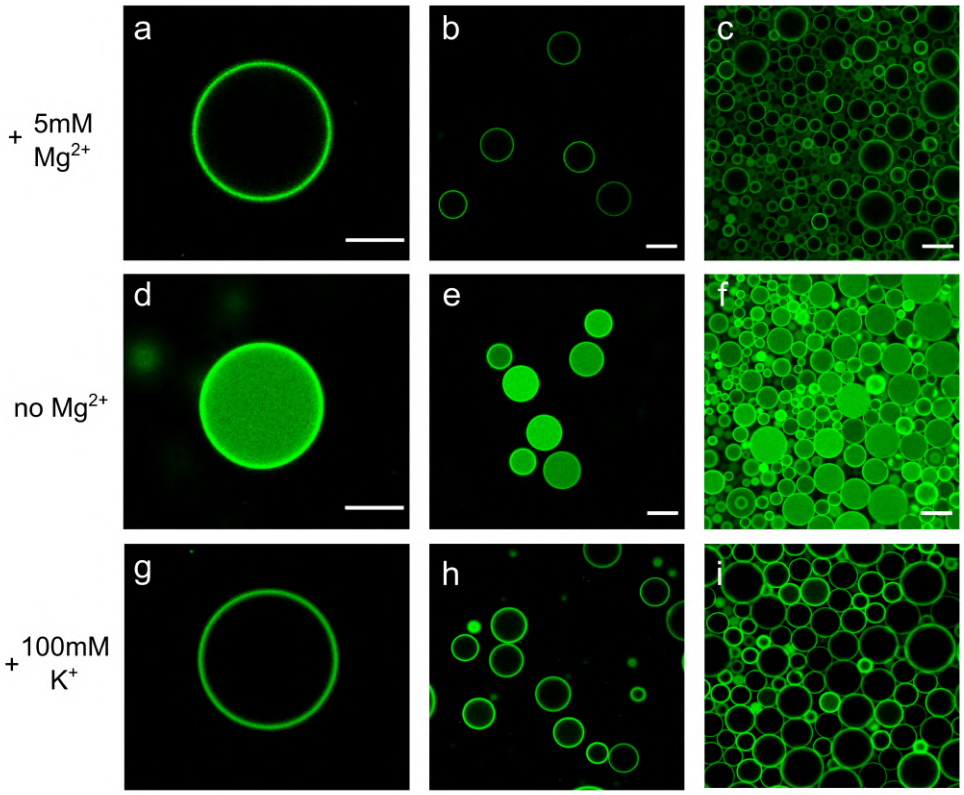

Supporting Figure 6: Influence of buffer conditions on the compartment functionalization with cholesterol-tagged DNA. Confocal fluorescence images of water-in-oil droplets with Atto488-labeled cholesterol-tagged DNA a-c) in 5 mM $MgCl_2$, 10 mM Tris-HCl, 1 mM EDTA, pH8; d-f) in 10 mM Tris-HCl, 1 mM EDTA, pH8; g-h) in 100 mM KCl, 10 mM Tris-HCl, 1 mM EDTA, pH8. The presence of magnesium ions or increased concentrations of potassium ions facilitates the binding of cholesterol-tagged DNA to the droplet periphery. Scale bars: a,d,g) 10 µm; b,c,e,f,h,i) 50 µm.

Figure S7: Stability of DNA-surfactant interaction over time

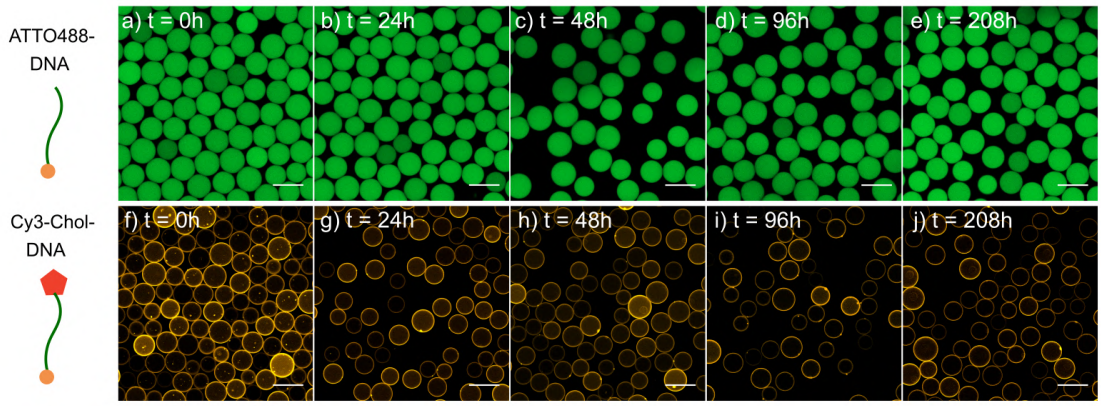

Supporting Figure 7: Cholesterol-tagged DNA remains stable at the droplet interface. a,b,c,d,e) Confocal fluorescence images of ATTO488-labeled cholesterol-free DNA encapsulated within water-in-oil droplets at 0 h, 24 h, 48 h, 96 h and 208 h; f,g,h,i,j) Confocal fluorescence images of cholesterol-tagged Cy3-labeled DNA encapsulated within water-in-oil droplets at 0 h, 24 h, 48 h, 96 h and 208 h. The cholesterol-free DNA remains homogeneously distributed in the droplet's lumen throughout several days, indicating both that there is no unspecific binding to the periphery and that the water-in-oil droplet remains stable. In contrast, the cholesterol-tagged DNA is only distributed along the droplets periphery showcasing the strong hydrophobic surfactant-cholesterol interaction. The aqueous phase contained 10 mM Tris-HCl, 1 mM EDTA, 5 mM $MgCl_2$, pH 8 and 4 µM DNA. Scale bars: 50 µm.

Text S1, Table S2: Interfacial tension measurements

A drop shape analyzer DSA25 (Krüss GmbH, Germany) tensiometer with CCD-camera and the pendant drop method was used to measure the surface tension at the interface of surfactants and aqueous phase in presence and absence of cholesterol-tagged DNA. The Laplace-Young equation was selected as a fitting-method.[4] Oil and aqueous phase densities were set to $1.6\,\mathrm{g\,cm^{-3}}$ and $0.99\,\mathrm{g\,cm^{-3}}$, respectively. For the measurements 1 mL of the aqueous phase (10 mM Tris-HCl, 1 mM EDTA, 5 mM $MgCl_2$, pH 8) was used in a plastic cuvette. To study to which extent cholesterol-tagged DNA alters the IFT, three solutions were investigated: one DNA-free, one with 2 µM cholesterol-tagged DNA (#1) and one with 2 µM cholesterol-tagged and complementary DNA – all in the standard buffer (Buffer 1). The oil phase contained either commercial surfactant (2 wt% of Perflouro-polyether-polyethylene glycol (PFPE-PEG) block-copolymer fluorosurfactants from Ran Biotechnologies, Inc.) or custom-synthesized surfactant (2.5 mM of a triblock-copolymer PFPE-PEG-PFPE triblock-copolymer surfactant[2,5]) diluted in HFE-7500 (DuPont). Prior to the measurement, samples were drawn into 1 mL syringes equipped with a cannula (0.8 mm x 22 mm blunt/dull) and lowered into the aqueous phase. Drops were created using the software controlled dosing unit. Droplet interfacial tension (IFT $[\mathrm{mN\,m^{-1}}]$) was analyzed over time. Once the IFT did not show any change, the measurement was stopped and the IFT was collected. For each surfactant/buffer experiment, three measurements were performed and the mean value as well as the standard deviation were calculated. All results are presented in Table S2.

Supporting Table 2: Interfacial tension between aquous and oil/surfactant phase for DNA-free aqueous solution (10 mM Tris-HCl, 1 mM EDTA, 5 mM $MgCl_2$, pH 8), or solutions where either 2 µM cholesterol-tagged DNA or 2 µM cholesterol-tagged DNA and 2 µM of its complementary strand have been added. The measurements have been carried out for both surfactants used in this study. The results indicate a small but insignificant change of the IFT between aqueous and oil phase. Nonetheless, a trend to lower tension can be deduced in the presence of cholesterol-tagged DNA.

Surfactant	DNA-free [$mN\,m^{-1}$]	Cholesterol-tagged DNA [$mN\,m^{-1}$]	Cholesterol-tagged and complementary DNA [$mN\,m^{-1}$]
Commercial	3.89 ± 0.07	3.78 ± 0.12	3.21 ± 0.10
Synthesized	4.72 ± 0.06	3.16 ± 0.27	2.09 ± 0.53

Text S2: FRAP analysis

For the FRAP analysis, normalized intensity values were calculated as follows:

$$I_{normalized} = \frac{I_{measured}}{I_{pre}}, \tag{1}$$

I_{pre} was calculated by taking the average of the five measured intensity values before bleaching. Due to the low number of acquired images, a correction for the bleaching of the dye during this pre-bleaching phase has not been taken into account. A non-linear least-square fit was applied to the normalized intensities from the recovery phase. The fit-function was of the form:

$$f(t) = A(1 - exp(-\lambda t)) + x_0, \tag{2}$$

where A and λ, are fit parameters and x_0 is the time point after bleaching i.e. the start of the recovery phase. With this, following the protocol of Axelrod[6] and Soumpasis,[7] the diffusion coefficient can be calculated via:

$$D = 0.32\frac{r^2}{\tau_{1/2}} = -0.32\frac{\lambda r^2}{0.5}, \tag{3}$$

where τ is the half-recovery time and r the radius of the circular bleaching spot (2.5 µm). In order to efficiently evaluate the measured data, a custom-written MATLAB script performing the above mentioned operations was used.

Text S3, Figure S8: Correlation between diffusion coefficient and surfactant concentration

In order to study the behavior of cholesterol-tagged DNA within the surfactant layer, we performed FRAP measurements for a variety of surfactant concentrations. The experiments were carried out with a commercial surfactant (008-FluoroSurfactant, RAN Biotechnologies). The results can be seen in Figure S5, which shows the diffusion coefficient as a function of surfactant concentration. The droplets were around 30 µm in diameter.

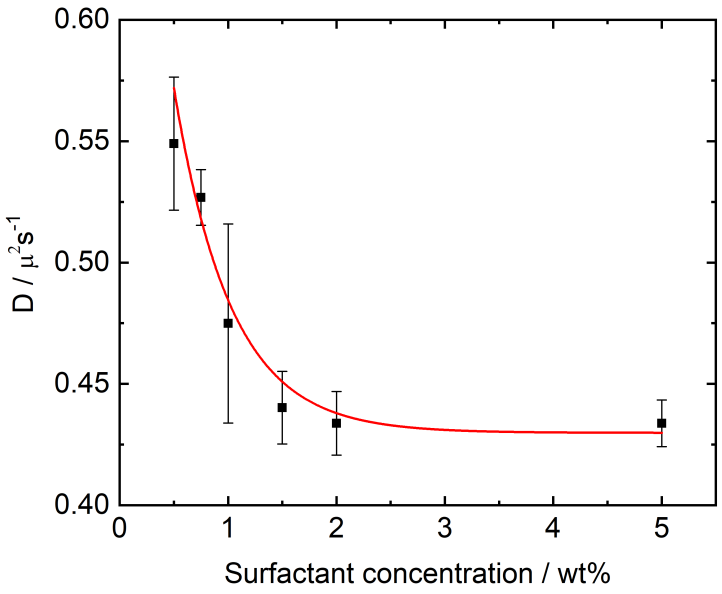

Supporting Figure 8: Diffusion coefficient of cholesterol-tagged Atto488-labelled DNA encapsulated in surfactant-stabilized droplets as a function of surfactant concentration (in weight percent). The error bars correspond to the standard deviation of at least 9 independent measurements. If the droplet moved during the acquisition interval, the recorded data was not taken into consideration. The data points were fitted with an exponential decay function (red curve).

The diffusion coefficient decreases with an increasing surfactant concentration. A nonlinear-least square fit has been applied using the formula:

$$D(c) = Aexp(-\lambda c), \tag{4}$$

where A and λ are fitting coefficients and c the surfactant concentration. A possible interpretation of this result is that the packing of the surfactants at the droplet periphery changes with the surfactant concentration. An increasing concentration results in a denser packing at the droplet periphery and therefore a decreased diffusion coefficient of the cholesterol-tagged DNA. It also makes sense that the packing of surfactants at the periphery is limited. As the data indicate, the diffusion coefficient remains constant above a surfactant concentration of 2 wt%. This could be due to the saturation of densely packed surfactant at the droplet periphery. It is possible that the insertion of cholesterol-tagged DNA into the surfactant layer provides an experimental handle to determine the diffusive properties of surfactants.[8]

Figure S9: Complementary DNA binding at the droplet periphery

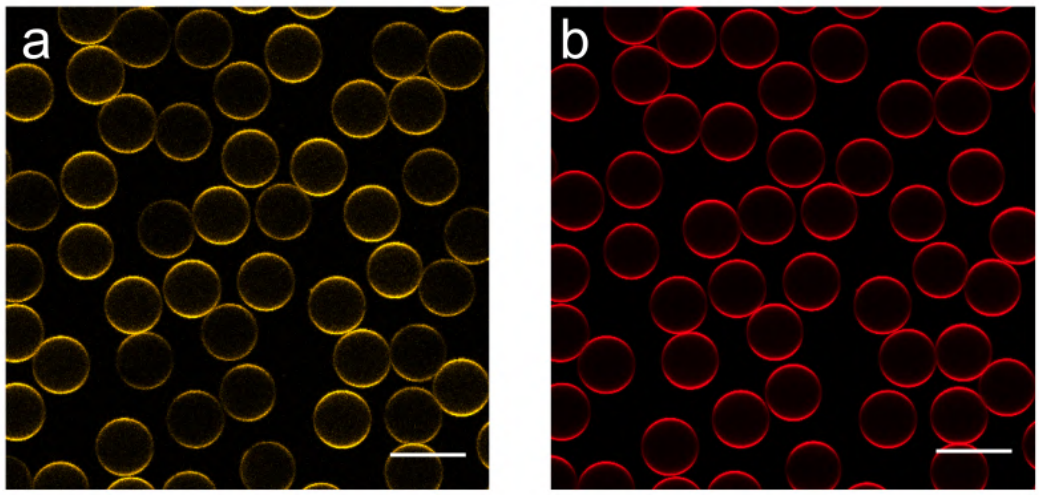

Supporting Figure 9: Confocal fluorescence imaging of droplets containing cholesterol-tagged DNA and a complementary DNA strand. a) Cholesterol-tagged DNA labeled with Cy3 at the droplet periphery; b) Complementary DNA labeled with Cy5 without a cholesterol-tag in the same water-in-oil droplets (containing 10 mM Tris-HCl, 1 mM EDTA, 5 mM $MgCl_2$, pH 8). The complementary DNA co-localizes with the cholesterol-tagged DNA, indicating successful DNA duplex formation. Scale bar: 50 µm.

Figure S10: FRAP with DNA-lattice

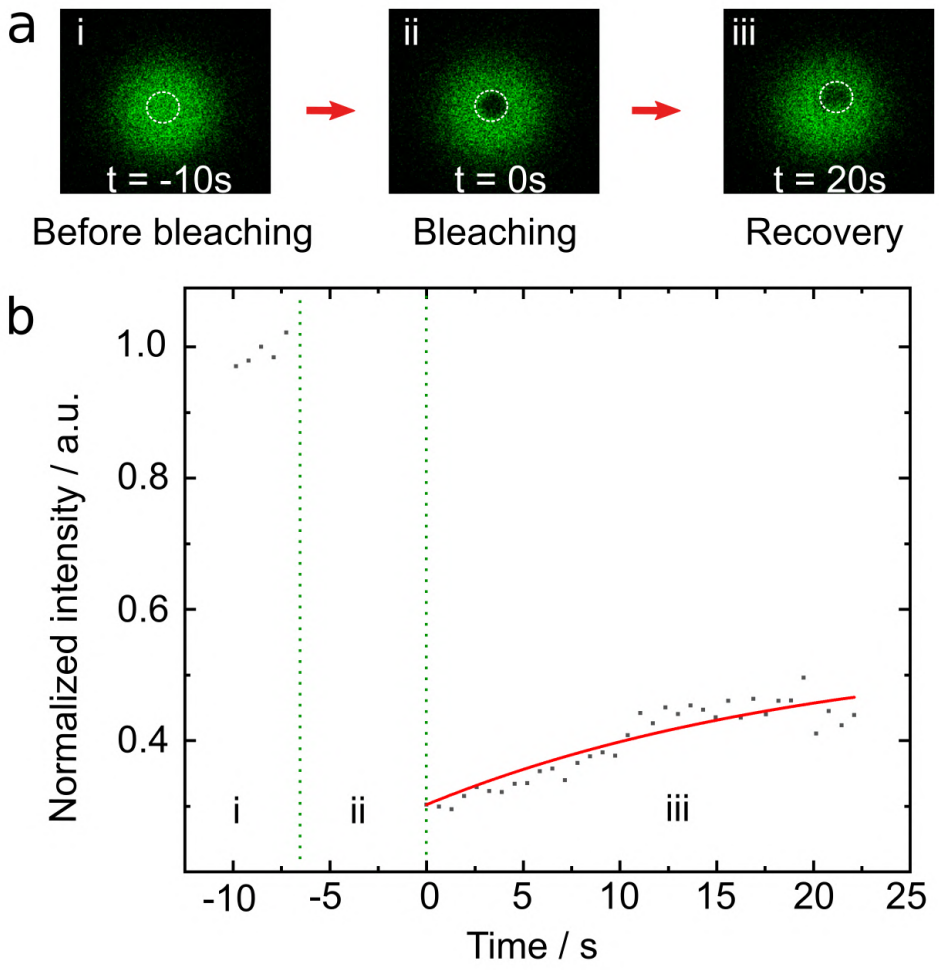

Supporting Figure 10: FRAP measurements of microfluidic water-in-oil droplets functionalized with a hexagonal DNA-lattice. a) Confocal fluorescence images of a droplet (bottom plane) i: before bleaching, ii: directly after bleaching (circular bleaching area clearly visible, $\lambda_{ex} = 488$nm), and iii: after recovery. The bleached area is highlighted with a white dashed circle. b) Representative recovery curve. Mean normalized intensity values within the bleaching area are plotted as a function of time. The red line represents an exponential fit, which was used to determine the diffusion coefficient, here: $D = 0.296\,\mu m^2\,s^{-1}$. The three phases of the experiment (i-iii) are indicated. The analysis of 18 droplets revealed a mean diffusion coefficient of $D = 0.33 \pm 0.03\,\mu m^2\,s^{-1}$, which is significantly lower than that of the cholesterol-tagged single-stranded DNA ($D = 0.41 \pm 0.01\,\mu m^2\,s^{-1}$).

Figures S11, S12, S13: Control experiments for microsphere attachment

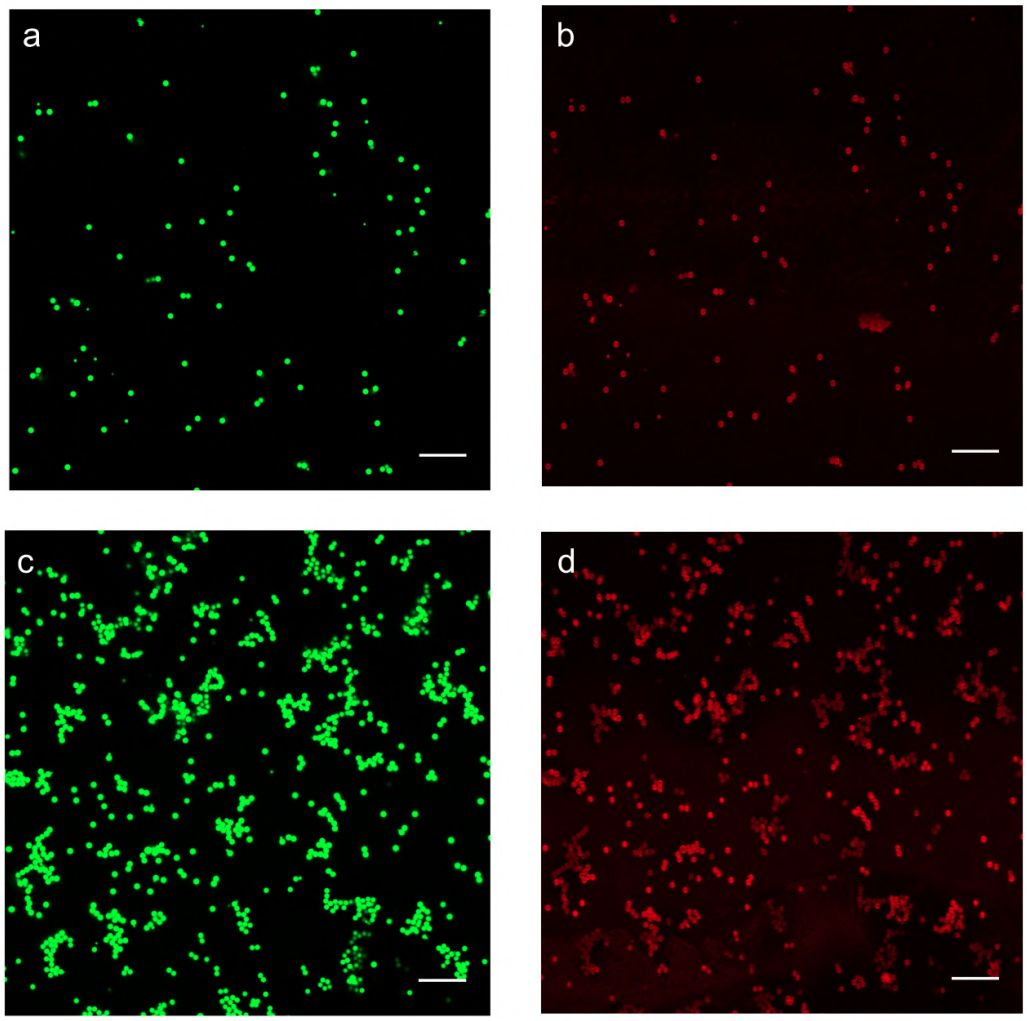

Supporting Figure 11: Cholesterol-tagged DNA binds polystyrene microspheres. a) Fluorescent (YG) microspheres in an aqueous solution (10 mM Tris-HCl, 1 mM EDTA, 5 mM $MgCl_2$, pH 8); b) Cy5-labeled DNA attached to the same beads via cholesterol-tagged DNA; c,d) Same as (a,b) but at a higher bead concentration, resulting in increased bead-bead interactions and clustering. Scale bar: 30 µm.

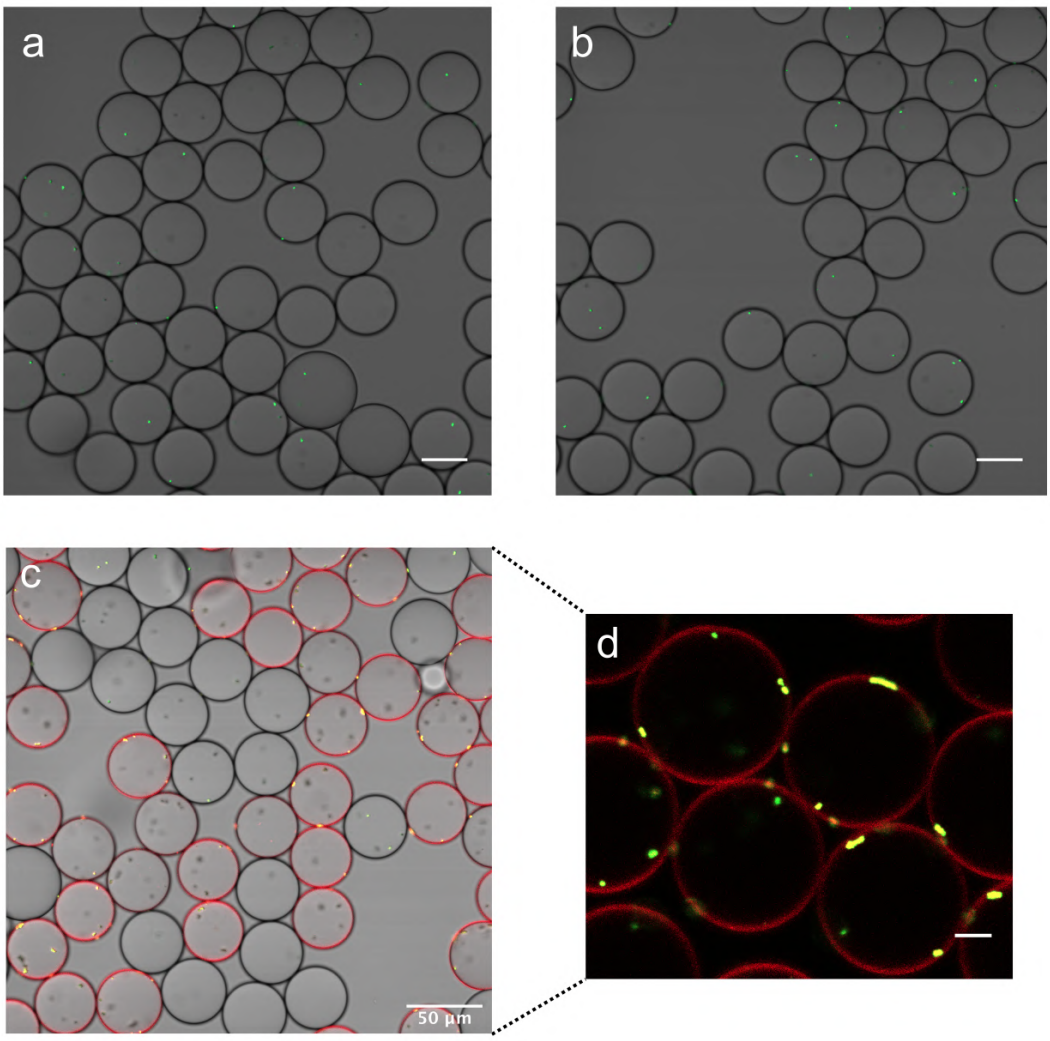

Supporting Figure 12: Functionalization of water-in-oil droplets with beads (diameter: 2 µm) via DNA-tags. a,b) Fluorescent (YG) microspheres (green) in water-in-oil droplets containing an aqueous solution (10 mM Tris-HCl, 1 mM EDTA, 5 mM $MgCl_2$, pH 8) without cholesterol-tagged DNA (control). For clarity, brightfield- and fluorescence images were overlaid. The beads were distributed randomly, neither favoring the droplet lumen nor its periphery. c,d) Fluorescent (YG) microspheres (green) in an aqueous solution containing cholesterol-tagged as well as a complementary Cy5-labeled DNA (red). In presence of DNA linkers, 95 % of the beads are localized at the periphery, whereas in their absence, we observe a random co-localisation of 23 %. Scale bar: 30 µm in a,b,c; 10 µm in d.

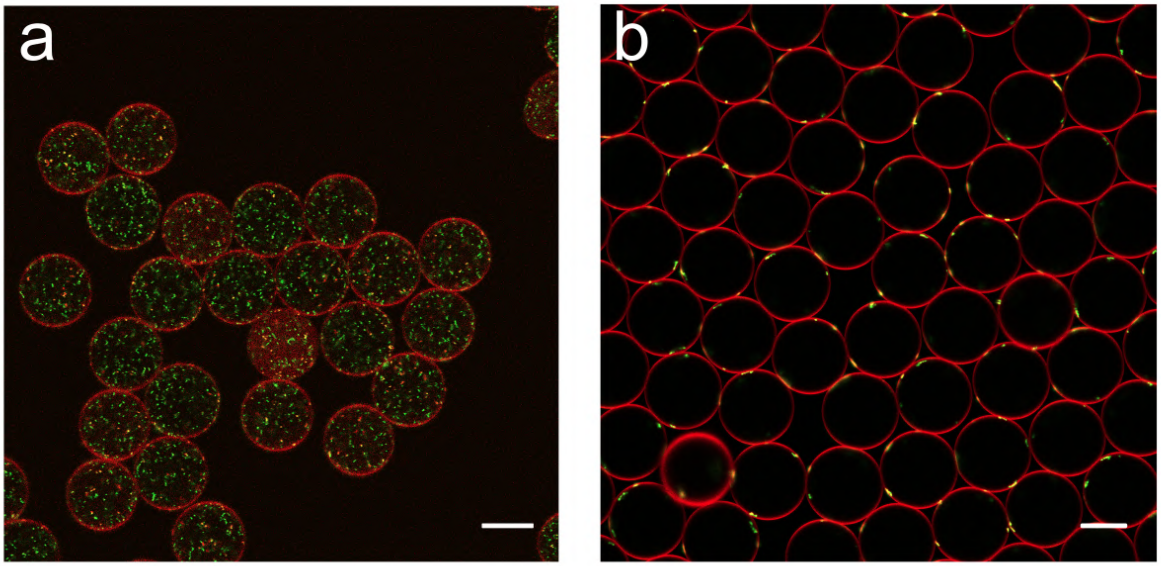

Supporting Figure 13: Functionalization of water-in-oil droplets with carboxylate-modified beads (diameter: 0.3 µm) via DNA-tags. a) Fluorescent (YG) carboxylate-modified microspheres (green) in water-in-oil droplets. The aqueous solution consists of 10 mM Tris-HCl, 1 mM EDTA, 5 mM $MgCl_2$, pH 8 with added DNA, namely cholesterol-tagged DNA and its complementary Cy5-labeled DNA (red) but without the interconnecting strand #8. For clarity, the fluorescence images were overlaid. The beads were distributed randomly, neither favoring the droplet lumen nor its periphery. b) Fluorescent (YG) microspheres (green) in an aqueous solution containing cholesterol-tagged DNA and its complementary Cy5-labeled DNA (red) as well as the interconnecting strand #8. The beads were localized at the droplet periphery. This opens up opportunities for diverse means of functionalizing droplets via modified beads. Scale bar: 30 µm.

Figure S14: Control experiments for actin cortex formation

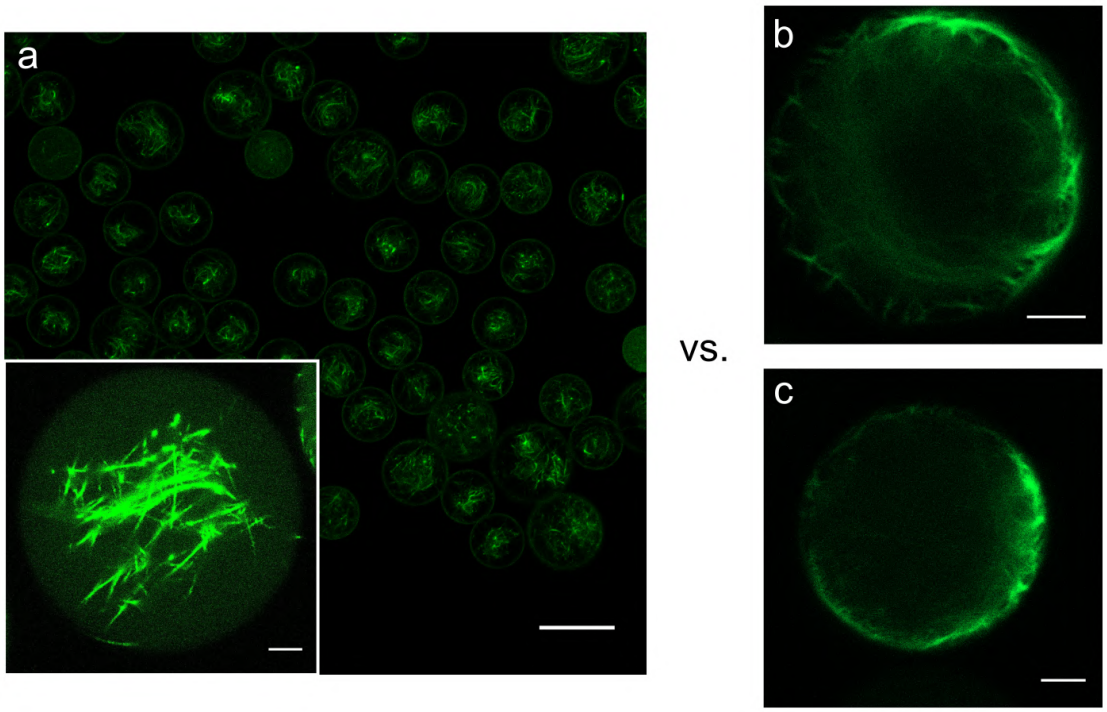

Supporting Figure 14: Formation of cortex-like actin structures inside droplets via DNA-tags. a) Filamentous (F-) actin inside surfactant-stabilized droplets without DNA. Actin filaments were distributed homogenously within droplets; b,c) F-actin inside surfactant-stabilized droplets with 10% biotinylated actin binding a strand of biotinylated DNA via streptavidin. The filaments are tethered to the droplet periphery via a complementary cholesterol-tagged DNA handle (like the one shown in Figure 3d). F-actin is found at the droplet interface. Scale bars: 50 µm in a) and 5 µm in the other images. For the actin polymerization protocol see the Material and Methods section in the main text.

Figure S15: Control experiments for attachment of leukemia cells

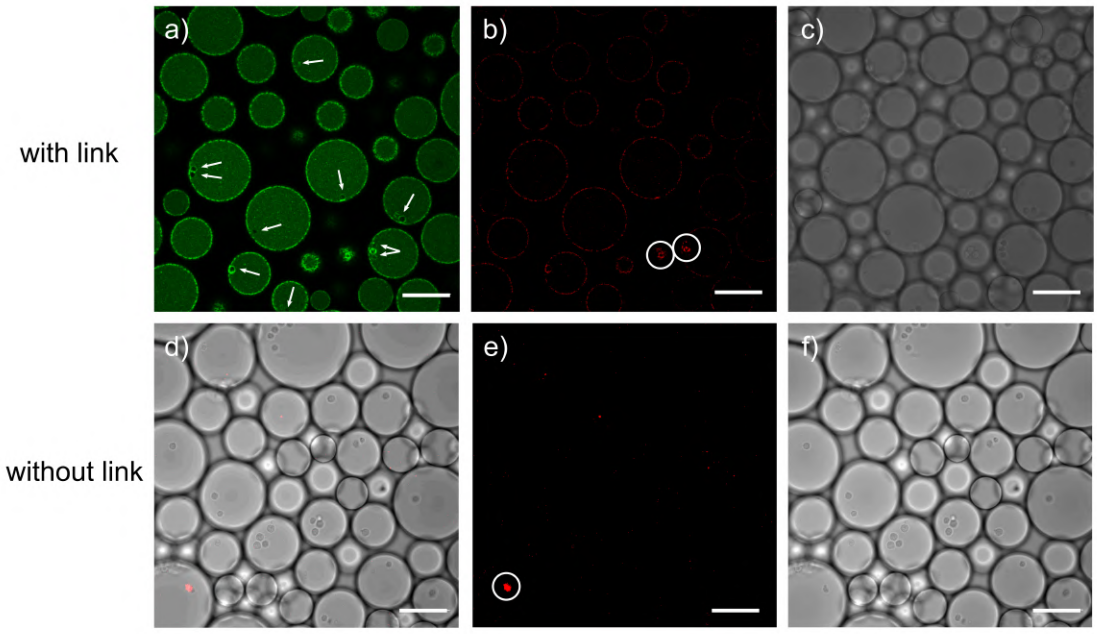

Supporting Figure 15: Leukemia cells can be linked to the droplet periphery via DNA. Top row: DNA-mediated attachment to the periphery a) Atto488=labeled (λ_{ex} = 488nm) complementary strand (white arrows indicate linked cells), b) propidium iodide (λ_{ex} = 514nm) to show the cells viability (circles indicate dead cells), c) corresponding brightfield image. Bottom row: Without DNA, the cells do not interact with the droplet periphery d) composite of brightfield and propidium iodide channels, e) propidium iodide (λ_{ex} = 514nm) to show the cells viability (circles indicate dead cells), f) corresponding brightfield image. Scale bars: 100 µm.

Figure S16: Cell viability assay

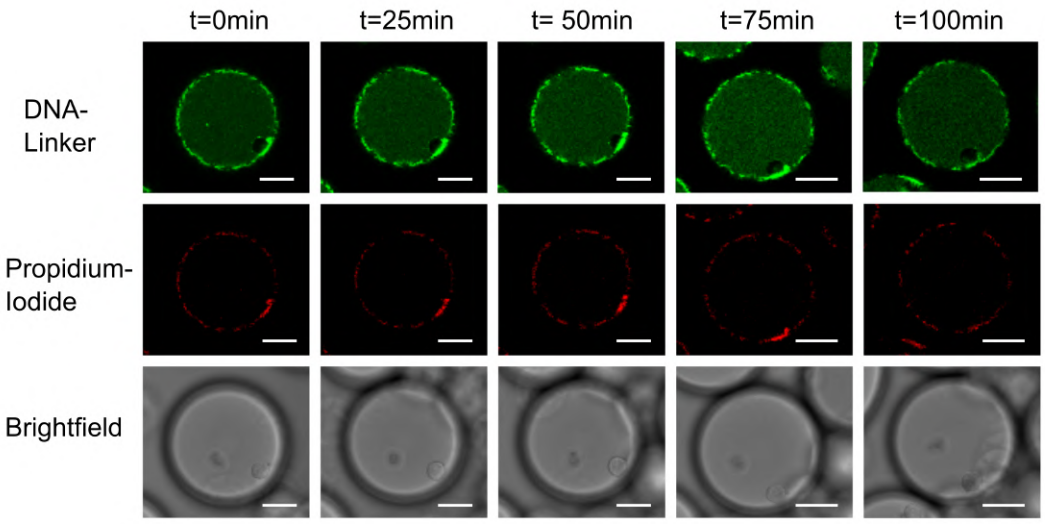

Supporting Figure 16: Cell viability assay for leukemia cells. An exemplary cell, incubated with complementary cholesterol-tagged DNA, over time in a solution of propidium iodide containing IMDM medium. Top row: Confocal fluorescence image of the complementary DNA-strand (λ_{ex} = 488nm). Middle row: Confocal fluorescence image of cell viability indicator propidium iodide (λ_{ex} = 514nm). Bottom row: Corresponding brightfield images. We found that 95% of the cells survive for more than 2 h, in the presence of cholesterol-tagged DNA and when encapsulated into droplets (139/146 alive). Scale bar: 30 µm.

Figure S17, S18, S19: Control experiments for attachment of T-lymphocytes

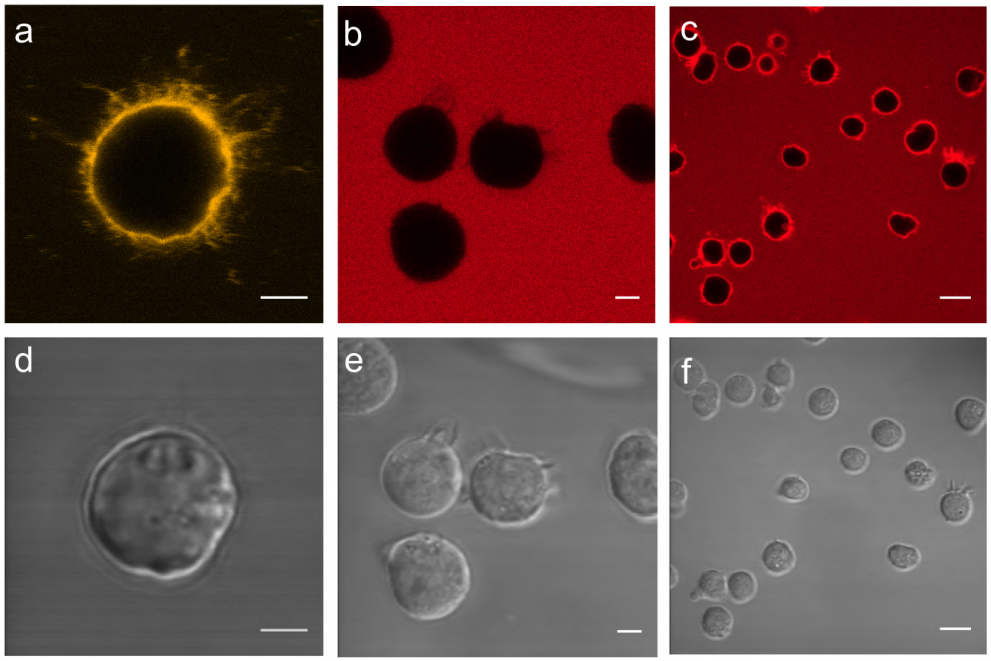

Supporting Figure 17: Cholesterol-tagged DNA attaches to Jurkat cells. a) Cy3-labeled cholesterol-tagged DNA mixed with the cell culture medium attached to the cell membrane; b) ROX-labeled DNA without a cholesterol-tag, added with the cell culture medium was homogeneously distributed in the extracellular space; c) The ROX-labeled strand attached to the cell periphery in the presence of its complementary cholesterol-tagged DNA strand; d-f) Corresponding brightfield images. Scale bars: 3 µm in a, b, d and e; 10 µm in c and f.

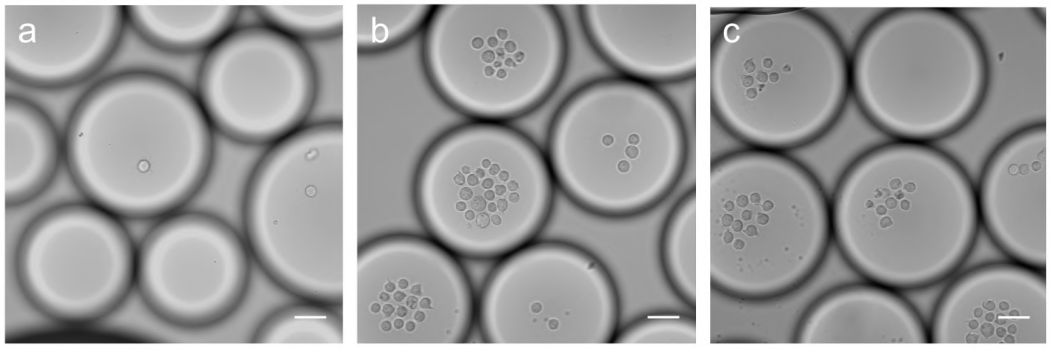

Supporting Figure 18: Jurkat cells are located at the bottom of surfactant-stabilized droplets in the absence of DNA linkers. a,b,c) Jurkat cells were encapsulated in droplets with RPMI cell culture medium without the addition of DNA. The cells sank to the bottom of the droplets indicating a lack of directed interaction with the droplet interface. This is the case both in single cells (a) and at higher cell concentrations (b,c). Scale bar: 30 µm.

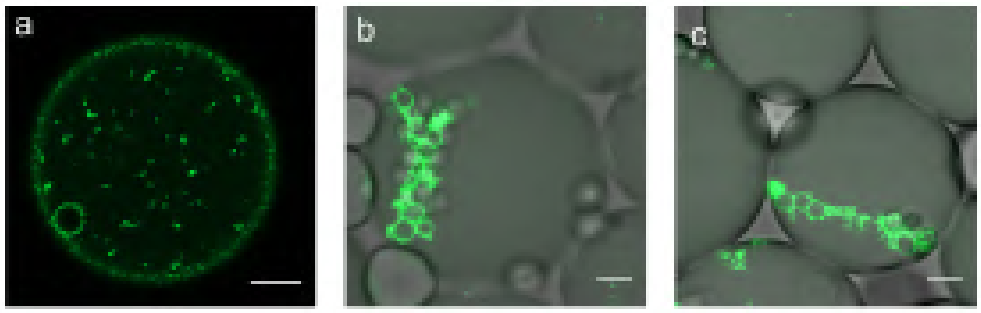

Supporting Figure 19: Jurkat cells can form droplet spanning multicellular clusters in the presence of the DNA linkers. a,b) A high concentration of Jurkat cells (10^7 per milliliter) encapsulated in droplets with RPMI cell culture medium together with the DNA linkers. A representative composite brightfield and fluorescence image (DNA is FITC-labeled) is shown. Higher cell and DNA concentrations result in an increase of cell-cell interactions, resulting in droplet-spanning multicellular clusters. Scale bar: 20 µm.

Text S4: Supporting videos

We performed high-speed fluorescence imaging (see Materials and Methods, main text) to investigate the kinetics of the interaction between cholesterol-tagged DNA and the compartment periphery. For this purpose, we imaged the droplets at the time of the production and at the outlet of the microfluidic device (see Figure S2).

Video S1: Video S1 shows the droplet production process at the microfluidic T-junction, encapsulating 10 µM Cy3-labeled cholesterol-tagged DNA via the aqueous inlet.

Video S2: Video S2 is taken during the same experiment as above, yet at the microfluidic outlet. The increased fluorescence intensity at the droplet periphery indicates that attachment happens within milliseconds – the time that the droplets need to travel from the point of production to the microfluidic outlet given the flow rates (oil flow rate: $120\,\mu l\,h^{-1}$; water flow rate: $30\,\mu l\,h^{-1}$) and the dimensions of the microfluidic device (distance between T-junction and outlet: 7 mm; channel width: 30 µm; channel height: 30 µm).

Video S3: Video S3 shows droplets containing 10 µM Cy3-labeled cholesterol-free DNA as a control. At the microfluidic outlet, the DNA remains homogeneously distributed.

Scale bar in all videos: 30 µm.

References

(1) Kurokawa, C.; Fujiwara, K.; Morita, M.; Kawamata, I.; Kawagishi, Y.; Sakai, A.; Murayama, Y.; ichiro M. Nomura, S.; Murata, S.; Takinoue, M.; Yanagisawa, M. *Proceedings of the National Academy of Sciences* **2017**, *114*, 7228–7233.

(2) Platzman, I.; Janiesch, J.-W.; Spatz, J. P. *Journal of the American Chemical Society* **2013**, *135*, 3339–3342.

(3) Weiss, M. et al. *Nature Materials* **2017**, *17*, 89–96.

(4) Girault, H.; Schiffrin, D.; Smith, B. *Journal of Electroanalytical Chemistry and Interfacial Electrochemistry* **1982**, *137*, 207 – 217.

(5) Janiesch, J.-W.; Weiss, M.; Kannenberg, G.; Hannabuss, J.; Surrey, T.; Platzman, I.; Spatz, J. P. *Analytical Chemistry* **2015**, *87*, 2063–2067.

(6) Axelrod, D.; Koppel, D.; Schlessinger, J.; Elson, E.; Webb, W. *Biophysical Journal* **1976**, *16*, 1055–1069.

(7) Soumpasis, D. *Biophysical Journal* **1983**, *41*, 95–97.

(8) Weinheimer, R. M.; Evans, D.; Cussler, E. *Journal of Colloid and Interface Science* **1981**, *80*, 357–368.